CAN EXPERIMENTS DISTINGUISH BETWEEN RADIATIVE ELECTROWEAK SYMMETRY BREAKING AND CONVENTIONAL BREAKING.

F. N. Ndili
Physics Department
University of Houston, Houston, TX.77204, USA.

August, 2007

Abstract

We present a comparative study of radiative electroweak symmetry breaking and conventional standard model breaking, and pose the question whether experiments can distinguish one breaking mode from the other. The importance of the problem lies in the fact that the two breaking modes have very different physical interpretations concerning the mechanism of spontaneous electroweak symmetry breaking and the origin of mass.

Keywords: Radiative Electroweak symmetry breaking
PACS: 12.38.-t,
E-mail: fndili@uh.edu

1 INTRODUCTION

Coleman and Weinberg pointed out several years ago [1] that quantum loops and radiative corrections can play an important role in determining the structure of the vacuum of a quantum field or system of fields and particles. Specifically they showed that while a scalar field with mass parameter $\mu^2 = 0$ and classical tree potential is unable to develop a vacuum expectation value (VEV) and spontaneous symmetry breaking (SSB), such VEV and SSB become achievable when we take quantum loops into account. This is particularly so if the scalar field is coupled to a gauge field and dimensional transmutation can occur. The overall conclusion is that an alternative electroweak symmetry breaking (EWSB) mechanism exists along side the standard model EWSB mechanism that is based on the classical tree potential:

$$V(\Phi) = \frac{1}{2}\mu^2\Phi^2 + \frac{\lambda}{4}\Phi^4 \tag{1}$$

with a non-zero negative mass parameter $\mu^2 < 0$. The Coleman-Weinberg alternative model dispenses with the mass parameter $\mu^2 = 0$ in equation (1) but adds quantum loops or higher order potential terms. This alternative mechanism has become known as radiative Electroweak symmetry breaking (REWSB).

The fact is that these two mechanisms do not just differ in what terms appear or do not appear in the scalar field potential, but lead to very different physical perceptions of what causes electroweak symmetry breaking. The standard model based on equation (1) with its $\mu^2 < 0$ attributes electroweak symmetry breaking to a primordial fundamental scalar field that unlike any existing particle known so far has a negative mass parameter $\mu^2 < 0$. In contrast, the Coleman-Weinberg REWSB mechanism would attribute EWSB to quantum dynamics and a quantum origin. Such quantum dynamics if favored would widen the scope for our search and understanding of EWSB and the origin of mass. Another way of looking at the matter is to say that in the standard model mechanism CEWSB, the quantum system starts off with a pre-assigned mass scale $\mu \neq 0$, compared to the Coleman-Weinberg model REWSB where the same quantum system is left to fix its own scale of dynamics. The question arises what role the pre-assigned scale parameter μ plays in the quantum dynamics, and whether we can find any observable features that distinguish the outcome of these two dynamics.

Because of the widely differing physical interpretations of the two mechanisms, we consider it worthwhile to examine in some quantitative detail,

what observational features and signatures distinguish REWSB on the one hand, from the conventional standard model electroweak symmetry breaking (CEWSB) on the other hand. Elias et. al. [2-6] have considered the problem from one perspective.

Our approach to the problem is to first set out in section 2, aspects of electroweak symmetry breaking that do not depend on any explicit choice of the scalar field potential $V(\Phi)$. Such aspects will therefore be common to both REWSB and CEWSB and we may call these aspects the core of electroweak symmetry breaking. Thereafter, we take up equation (1) in section 3, with its $\mu^2 < 0$, as one explicit choice of the scalar potential. Then we work out what new relations besides the core EWSB equations, follow from this one choice of $V(\Phi)$. These new relations or features we can call the specific signatures of the standard model CEWSB. In section 4, we make a different choice of the scalar potential, by setting $\mu^2 = 0$ which is the Coleman-Weinberg REWSB model, with quantum loops added. We work out the new features in relation to the core equations, and call these the signatures of REWSB. We proceed further in sections 5 and 6, to re-examine the same REWSB using the more modern aspects of the Coleman-Weinberg model known as the renormalization group improved effective potential [7-10]. Further improvement using 2-loop β and γ functions is considered in section 7. The two sets of signatures, CEWSB and REWSB, are compared in section 8. Our final results and conclusions are stated in section 9.

2 Core relations of electroweak symmetry breaking

In terms of a scalar field, the core features that break electroweak symmetry even when no explicit scalar potential is specified, are a complex scalar field that may or may not be a fundamental field. This complex scalar field must be a doublet under the electroweak $SU(2)_L \times U(1)_Y$ gauge symmetry. The complex doublet scalar field must have a non zero vacuum expectation value we take to be v. Given such a field one is able to immediately write or parameterize it in the form:

$$\Phi = \begin{pmatrix} \Phi^+ \\ \Phi^o \end{pmatrix} = \begin{pmatrix} \phi_1^+ + i\phi_2^+ \\ \phi_3^o + i\phi_4^o \end{pmatrix} = e^{i\xi(x).\tau/v} \begin{pmatrix} 0 \\ \frac{v+h(x)}{\sqrt{2}} \end{pmatrix} \tag{2}$$

in which only one component field ϕ_3^o acquires the non-zero vacuum expectation value written:

$$\langle \Phi \rangle = \langle \phi_3^o \rangle = \frac{v}{\sqrt{2}} \tag{3}$$

This form of the scalar field is all that is required to derive many results and features of the EWSB. These several features include various charged and neutral currents as well as couplings of fermions and gauge bosons to the scalar field. The details of these core features can be seen in several places such as [11]. Among these relations that we obtain without our specifying any explicit scalar potential, are the gauge boson masses :

$$M_W^2 = \frac{g_2^2 v^2}{4} \tag{4}$$

$$M_Z^2 = \frac{v^2(g_2^2 + g_1^2)}{4} \tag{5}$$

where g_2 is $SU(2)_L$ coupling constant, and g_1 is $U(1)_Y$ coupling constant.

It turns out also that a definitive numerical value of v = 246 GeV can be obtained without recourse to any explicit choice of the scalar potential. One simply combines the V-A current structure of the gauge theory [11], with such accessible processes as μ decays, and obtains expression for v in terms of the Fermi constant :

$$v = 2^{-1/4} G_F^{-2} = 246 GeV. \tag{6}$$

Given this value of v and the known masses of the gauge bosons stated in equations (4) and (5), one deduces the values of the two gauge coupling constants at the EWSB scale v:

$$g_2 = 0.6585; g_1 = 0.3407 \tag{7}$$

Similarly from Yukawa couplings of equation (2) to fermions, we obtain fermion mass relations and couplings:

$$m_f = \frac{g_f v}{\sqrt{2}} \tag{8}$$

where g_f stands for Yukawa coupling constant of a given fermion f, such as the top quark g_t. Again these relations do not require any explicit choice or specification of the scalar potential. In particular, the relations hold whether $\mu = 0$ as in REWSB, or $\mu \neq 0$ (CEWSB).

We now note one area where we are not able to obtain any information at all based on equation (2) alone, without specifying some explicit form of the scalar potential. This area is in the determination of physical Higgs particle mass m_h, and the self coupling parameter λ of the scalar field and its components. This becomes the area where we can focus our search for any distinguishing features between REWSB and CEWSB. We will therefore proceed by devising ways to determine these two quantities m_h and λ, first in a CEWSB model and then in a REWSB model. Both quantities turn out to be derivable from some explicit form of the scalar potential we now write as $V(\phi)$ where ϕ stands for the scalar field (component) that has the non-zero VEV. Our main focus is in the structure and analysis of such two potentials V_{CEWSB} and V_{REWSB}, and the Higgs masses and couplings they predict.

3 Conventional Standard Model Potential CEWSB

The conventional EWSB is based on equation (1). This potential defines the ground state of the system

$$\frac{dV(\phi)}{d\phi(x)} = 0 \tag{9}$$

and gives a value of the VEV of ϕ in terms of the parameters of the chosen potential :

$$\langle\phi(x)\rangle = \frac{v}{\sqrt{2}} = \sqrt{\frac{-\mu^2}{\lambda}} \tag{10}$$

with $\mu^2 < 0$. Upon plugging equations (2) and (10) into equation (1), we obtain a mass relation for the physical Higgs particle h(x): It is :

$$m_h^2 = -2\mu^2 \tag{11}$$

More formally the mass of the Higgs particle is given in terms of a chosen potential by:

$$\frac{d^2V(\phi)}{d\phi^2}|_{\phi=v/\sqrt{2}} = m_h^2 \tag{12}$$

Equations (10) and (11) become new relations which used separately or in combination with the core equations (2) - (8) may lead to specific signatures of the CEWSB. Thus from equations (10) and (11) we get

$$m_h^2 = -2\mu^2 = \lambda v^2 \tag{13}$$

as a relation specific to CEWSB model. We can go further to use the core value v = 246 GeV and relate m_h specifically to λ as:

$$m_h = 246\sqrt{\lambda} \tag{14}$$

If we assume that the scalar field interaction was perturbative
in the dynamics leading to EWSB at scale v, and that $\lambda \leq 1$, we obtain that : $m_h \leq 246GeV$ which becomes a signature of CEWSB mechanism. On the other hand, if $\lambda > 1$, then CEWSB predicts $m_h > 246$ GeV. Notably however, the CEWSB does not give us any specific value for Higgs mass nor a value for λ.

4 The Coleman Weinberg REWSB Potential

We consider next the Coleman Weinberg REWSB potential and what signatures we can tag onto it. For a $\lambda\phi^4$ scalar field theory, Coleman and Weinberg obtained the general expression for its effective potential:

$$V_{eff}(\phi_c) = -\sum_n^{\infty} \frac{1}{n!}\Gamma^{(n)}(00....0)[\phi_c(x)]^n \tag{15}$$

where ϕ_c is the classical field that has non-zero vacuum expectation value. $\Gamma^{(n)}(00...0)$ are 1PI vertex Greens functions to which n external legs $[\phi_c(x)]^n$ attach, each carrying zero momentum. When these 1PI functions are expanded perturbatively into Feynman loops, the above series can be re-organized into a perturbative loop expansion for the same effective potential:

$$V_{eff}(\phi) = V_o + V_{1L}(\phi) + V_{2L}(\phi) + ... \tag{16}$$

where V_o is the tree potential given by equation (1); V_{1L} is the one-loop potential; V_{2L} is the 2-loop potential, etc. The above loop potentials require in general to be renormalized. The renormalized effective potential determines the state of EWSB and the Higgs mass through the standard equations:

$$\frac{dV(\phi)}{d\phi}|_{\phi=v/\sqrt{2}} = 0 \tag{17}$$

$$\frac{d^2V(\phi)}{d\phi^2}|_{\phi=v/\sqrt{2}} = m_h^2 \tag{18}$$

$$\frac{d^4V(\phi)}{d\phi^4}|_{\phi=v/\sqrt{2}} = 6\lambda \tag{19}$$

For a purely scalar field theory, the above loops involve only virtual scalar particles. When however other fields are present in the system that can couple radiatively to the scalar field, the loop contributions of these other fields to $V_{eff}(\phi_c)$ have to be taken into account. In the specific case of EWSB where fermions and gauge bosons are present besides the scalar field, the Coleman Weinberg potential generalizes to include quarks, leptons and gauge boson loops. These extended loop calculations have been carried out in a number of places [7, 11]. We write down some of the results up to 1-loop potential for REWSB. In one form Cheng and Li write [11]:

$$V_{eff}(\phi) = V_o + V_{1L}(\phi) = \frac{\lambda}{4}\phi^4 + C(log\frac{\phi^2}{M^2} + ...) \tag{20}$$

where M^2 is the renormalization scale; and C is given by:

$$C = \frac{1}{64\pi^2}[3\sum_v m_v^4 + m_s^4 - 12\sum_f m_f^4] \tag{21}$$

Here m_v are vector boson masses (W^+, W^-, Z^o); $m_s = m_h$ is scalar (physical Higgs) boson mass, and m_f are the fermion masses, quarks and leptons.

Using core equations (4)-(8) without using any equations from CEWSB section 3, we can rewrite equation (21) in terms of coupling constants as follows:

$$C = \frac{\phi^4}{64\pi^2}\left[\frac{3(3g_2^4 + 2g_2^2g_1^2 + g_1^4)}{16} + 12\lambda^2 - \sum_f 3g_f^4\right] \tag{22}$$

If we neglect contributions from all leptons and quarks except the top quark, we can write the REWSB potential equation (20) up to 1-loop potential finally as [2] :

$$V_{eff}(\phi) = \frac{\lambda\phi^4}{4} + \phi^4\left[\frac{12\lambda^2 - 3g_t^4}{64\pi^2} + \frac{3(3g_2^4 + 2g_2^2g_1^2 + g_1^4)}{1024\pi^2}\right](log\frac{\phi^2}{M^2} - \frac{25}{6}) \tag{23}$$

Here g_t is the top quark loop Yukawa coupling. The neglect of other fermion couplings follows from equation (8), where a fermion Yukawa coupling is proportional to its mass, and the top quark with its dominant mass clearly overshadows all other fermions. Regarding the parameter M in the above equation, we note that in the absence of a pre-set mass scale $\mu^2 = 0$ in the REWSB system, the quantum dynamics sets its own scale which we take to be the renormalization scale M, as well as the scale of any SSB in the system. Therefore we can re-define our renormalization conditions on the effective potential as ;

$$\frac{dV(\phi)}{d\phi}|_{\phi=M} = 0 \tag{24}$$

$$\frac{d^2V(\Phi)}{d\Phi^2}|_{\phi=M} = m_h^2 \tag{25}$$

$$\frac{d^4V(\Phi)}{d\Phi^4}|_{\phi=M} = 6\lambda \tag{26}$$

In place of equation (23), we can also write the 1-loop effective potential in the form due to Ford et.al. [8], and to Casas et. al.[9-10].

$$\begin{aligned} V_{eff}^{RG} &= \frac{6g_2^4\phi^4}{1024\pi^2}\left(log\frac{g_2^2\phi^2}{4M^2} - \frac{5}{6}\right) \\ &+ \frac{3g_2^4 + 6g_2^2g_1^2 + 3g_1^4}{1024\pi^2}\phi^4\left(log\frac{(g_2^2+g_1^2)\phi^2}{4M^2} - \frac{5}{6}\right) \\ &- \frac{3g_t^4\phi^4}{64\pi^2}\left(log\frac{g_t^2\phi^2}{2M^2} - \frac{3}{2}\right) \\ &+ \frac{9\lambda^2\phi^4}{256\pi^2}\left(log\frac{3\lambda\phi^2}{2M^2} - \frac{3}{2}\right) \\ &+ \frac{3\lambda^2\phi^4}{256\pi^2}\left(log\frac{\lambda\phi^2}{2M^2} - \frac{3}{2}\right) + \Omega \end{aligned} \tag{27}$$

We will work with the form (23). We plug equation (23) into equations (24) - (26) and obtain relations that embody REWSB signatures:

$$\frac{dV(\phi)}{d\phi}|_{\phi=M} = \lambda - \frac{44}{3}C = 0 \tag{28}$$

Putting C value from equation (22) we obtain a quadratic equation for λ:

$$\lambda^2 - \left(\frac{4\pi^2}{11}\right)\lambda - \frac{g_t^4}{4} + \frac{3g_2^4 + 2g_2^2g_1^2 + g_1^4}{64} = 0 \tag{29}$$

Using the core coupling values from equation (7), the quadratic equation becomes:

$$\lambda^2 - 3.588941\lambda - \frac{g_t^4}{4} + 0.0105973 = 0 \tag{30}$$

This gives two possible values of λ in terms of top quark Yukawa coupling constant g_t, both at the renormalization scale M = $\langle\phi\rangle = v/\sqrt{2}$:

$$\lambda = 1.794470496 + \sqrt{3.204151685 + \frac{g_t^4}{4}} \tag{31}$$

and

$$\lambda = 1.794470496 - \sqrt{3.204151685 + \frac{g_t^4}{4}} \tag{32}$$

If we require that both coupling constants are positive : $\lambda > 0; g_t > 0$, then solution (31) implies that $\lambda \gg g_t$ with $\lambda = 3.584485$ at $g_t = 0$. On the other hand, based on equation (32), we find at $g_t = 0, \lambda = 0.004456$, while for λ decreases to zero, $g_t = 0.50276$. This solution would indicate that the scalar dynamics in the EWSB has a coupling constant λ that lies between zero and a value 0.004456 while the Yukawa top quark coupling has a value that lies between zero and 0.502758496. We may take the mean of each parameter as its value at the EWSB scale in this case of solution (32). Then analogous to equation (7) we can write the λ and g_t values at the EWSB scale for solution (32) as :

$$\lambda = 0.002278; \frac{\lambda}{4\pi^2} = 5.77 \times 10^{-5}; g_t = 0.25138; \frac{g_t^2}{4\pi^2} = 5.07 \times 10^{-4}. \quad (33)$$

In this way, we may claim that solution (32) represents a situation where $g_t > \lambda$ at EWSB, while solution (31) represents a situation where $\lambda \gg g_t$ at EWSB scale. These two situations we can also try to distinguish in our signature analysis of REWSB.

In the case of solution (31), we can use the known top quark mass of 175 GeV along side equation (8) to estimate g_t at EWSB scale. We get that $g_t = 1.00605$, giving a corresponding value of λ from equation (31):

$$\lambda = 3.65464602; \frac{\lambda}{4\pi^2} = 0.092573; g_t = 1.00605; \frac{g_t^2}{4\pi^2} = 0.025637 \quad (34)$$

As seen from equations (33) and (34) both solutions (31) and (32) are perturbative, if we define perturbativity condition as:

$$\frac{\lambda}{4\pi^2} < 1; \frac{g_t^2}{4\pi^2} < 1. \quad (35)$$

The two solutions differ however in a profound way. This is that if the dynamics of EWSB is very weakly perturbative (both λ and h_t very small) as per equations (32) and (33), REWSB predicts that the top quark coupling is relatively much stronger than the scalar self interaction λ at the EWSB scale. On the other hand, if the EWSB dynamics is more strongly coupled, (both λ and g_t large), though still perturbative as per equations (31) and (34), the scalar self coupling constant λ is relatively much larger than the top quark Yukawa coupling constant g_t. These signatures of the REWSB can be ascertained experimentally.

We can go further to analyze equations (25) and (23) for Higgs mass. We obtain:

$$\frac{d^2V(\phi)}{d\phi^2}|_{\phi=M} = 3\lambda v^2 - 36Cv^2 = m_h^2 \tag{36}$$

Using $\lambda = (44/3)C$ from equation (28), this becomes:

$$m_h^2 = 8v^2C = 8v^2\left[\frac{12\lambda^2 - 3g_t^4}{64\pi^2} + \frac{3(3g_2^4 + 2g_2^2g_1^2 + g_1^4)}{1024\pi^2}\right] \tag{37}$$

Using core values from equation (7) we can rewrite equation (37) as:

$$m_h^2 = \frac{3v^2}{8\pi^2}\left[4\lambda^2 - g_t^4 + 0.042389076\right] \tag{38}$$

Next we use equation (31) or (32) to eliminate λ. We obtain:

$$m_h^2 = \frac{3v^2}{8\pi^2}\left[4\left(1.794470496 \pm \sqrt{3.204151685 + \frac{g_t^4}{4}}\right)^2 - g_t^4 + 0.042389076\right] \tag{39}$$

Finally using core equations (7) and (8) we obtain a Higgs boson mass for the REWSB model :

$$m_h^2 = \frac{3v^2}{8\pi^2}\left[4\left(1.794470496 \pm \sqrt{3.204151685 + \frac{m_t^4}{v^4}}\right)^2 - \frac{4m_t^4}{v^4} + 0.042389076\right] \tag{40}$$

Taking a top quark mass $m_t = 175GeV$ this evaluates to $m_h = 347.388GeV$, (the positive value). This appears high.

5 Renormalization group improved Effective potentials.

The Coleman-Weinberg 1-loop effective potential equation (23) used in the above analysis of REWSB, has the feature that it was defined at one and only one arbitrarily chosen mass scale point M which is the renormalization scale of the otherwise divergent effective potential. This one scale point M had also to be chosen as the EWSB point $\langle\phi\rangle = v/\sqrt{2} = M$, with $v = 246GeV$. This restricted choice of $\phi(x)$ was necessitated by the need for the log terms in equations (23) - (27) to vanish or remain small and perturbative. This feature of the Coleman-Weinberg potential equation (23) remains even if we

make another arbitrary choice of the renormalization point M'. We remain bound to study our effective potential and its signature values, only for field values ϕ in the vicinity of an arbitrarily chosen renormalization scale M. In effect, $V_{eff}(\phi(x))$ cannot be studied generally as a function of Higgs field $\phi(x)$ to ascertain how the potential behaves in these other regions of larger or smaller ϕ, and to what extent any new features such as new minima or maxima of $V_{eff}(\phi)$ found in those regions, affect or modify the EWSB features or signatures of V_{eff} found from earlier limited observation at one arbitrary renormalization point M. A way out of the problem is to free V_{eff} of its dependence on the renormalization scale M. That is we make V_{eff} a physical observable, whose field ϕ and coupling constant parameters λ_i can now vary widely over any desired domains, unaffected by any one arbitrarily chosen renormalization point M. Of course this freedom of the parameters of V_{eff} to vary widely still calls for some restraint such that the perturbative character of the overall loop expansion equations (15) and (16) can still be guaranteed. Both objectives and the automatic summing up of leading logarithms, are achieved by making the entire effective potential equation (15) or (16), satisfy a Renormalization Group equation(RGE) given by:

$$\left[M\frac{\partial}{\partial M}+\beta_\lambda\frac{\partial}{\partial\lambda}+\sum_i\beta_i\frac{\partial}{\partial g_i}-\gamma\phi\frac{\partial}{\partial\phi}\right]V_{eff}(M,\lambda,g_i,\phi..)=0 \qquad (41)$$

Here β_λ, β_i, and γ, are the RG functions (the beta functions and the anomalous dimension γ of the Higgs field). This RGE has a standard solution we write in the form :

$$V_{eff}^{RG}=V(M(t),\lambda(t),g_i(t),\phi(t)...) \qquad (42)$$

and call the RG improved effective potential. All its parameters $M(t), \lambda(t), g_i(t), \phi(t)...$, vary or run widely, each in a coordinated manner prescribed by its beta or gamma function. The variable t parameterizes the arbitrary renormalization scale, while the parameters of V_{eff}^{RG} run according to the equations:

$$M(t)=M_o e^t \qquad (43)$$

$$\phi(t)=\phi_o\xi(t)=\phi_o exp\left(-\int_0^t\gamma(\lambda(t');g_i(t'))dt'\right) \qquad (44)$$

with:

$$\gamma(t')=\sum_{n=1}^{\infty}\gamma^{(n)}(t'). \qquad (45)$$

Also:

$$\frac{d\lambda(t)}{dt}=\beta_\lambda(\lambda(t);g_i(t))=\sum_{n=1}^{\infty}\beta_\lambda^{(n)}. \qquad (46)$$

$$\frac{dg_i(t)}{dt} = \beta_{g_i}(g_i(t);\lambda) = \sum_{n=1}^{\infty} \beta_{g_i}^{(n)}. \tag{47}$$

In the above equations, M_o is some fixed initial renormalization point or reference scale, which we shall choose as $M_o = M_Z = 91.2GeV$, the Z^o gauge boson mass. Similarly the value of the Higgs field ϕ_o at $t = 0$ we shall choose as the field with VEV $\langle\phi_o\rangle = v/\sqrt{2}$ where $v = 246$ GeV. The beta and gamma functions have to be calculated separately to some loop order, and plugged into the above running equations. Explicit expressions of these β_i and γ functions computed to 1-loop and 2-loop orders for the EWSB system, have been tabulated by Ford et al. [8]. We shall rely on their values to compute numerically the parameters $\xi(t), \lambda(t), g_i(t)$ defined in equations (43)-(47).

In order to solve these integral and differential equations, we require to specify the boundary conditions of the equations. These boundary conditions are the values of the parameters at some chosen scale we specify as $t = 0$ which means scale $M = M_0 = M_Z = 91.2$GeV. Our explicit values of these parameters at $t = 0$ we take from equations (7), (33) and (34).

Once we have computed the explicit details of how the parameters vary with t over a wide range of values in equations (43) - (47), our aim will be to use the new RG improved effective potential equation (42) to re-examine the issue of signatures of REWSB. To proceed with the analysis, we need first to expand equation (42) into perturbative loop series and truncate the series at a convenient loop order chosen here as 1-loop order. Thus by analogy with equations (16) and (20), we write our RG improved effective potential equation (42) as:

$$V_{eff}^{RG}(\phi) = V_o^{RG}(\phi) + V_{1L}^{RG}(\phi) + V_{2L}^{RG}(\phi) + ... \tag{48}$$

To 1-loop order we write the RG improved REWSB potential as:

$$V_{eff}^{RG} = \frac{\lambda(t)\phi^4(t)}{4} + \phi^4(t)\left[\frac{12\lambda^2(t) - 3g_t^4(t)}{64\pi^2} + \frac{3(3g_2^4(t) + 2g_2^2(t)g_1^2(t) + g_1^4(t))}{1024\pi^2}\right](log\frac{\phi^2(t)}{M^2(t)} - \frac{25}{6}) \tag{49}$$

which replaces equation (23). Similarly, corresponding to equation (27) we would now write the RG improved 1-loop potential of Ford et. al. [8] and Casas et. al. [9-10]:

$$V_{eff}^{RG} = \frac{6g_2^4(t)\phi^4(t)}{1024\pi^2}\left(log\frac{g_2^2(t)\phi^2(t)}{4M^2} - \frac{5}{6}\right)$$

$$+\frac{3g_2^4(t)+6g_2^2(t)g_1^2(t)+3g_1^4(t)}{1024\pi^2}\phi^4(t)\left(log\frac{(g_2^2(t)+g_1^2(t))\phi^2(t)}{4M^2(t)}-\frac{5}{6}\right)$$
$$-\frac{3g_t^4(t)\phi^4(t)}{64\pi^2}\left(log\frac{g_t^2(t)\phi^2(t)}{2M^2(t)}-\frac{3}{2}\right)$$
$$+\frac{9\lambda^2(t)\phi^4(t)}{256\pi^2}\left(log\frac{3\lambda(t)\phi^2(t)}{2M^2(t)}-\frac{3}{2}\right)$$
$$+\frac{3\lambda^2(t)\phi^4(t)}{256\pi^2}\left(log\frac{\lambda(t)\phi^2(t)}{2M^2(t)}-\frac{3}{2}\right). \quad (50)$$

We will work with equation (49), and comment on equation (50) later. Our analysis of equation (49) now proceeds in stages as follows.

First we note that by construction the full (untruncated) RG improved effective potential equation (42) or (48) becomes independent of scale, satisfying :

$$\frac{dV_{eff}^{RG}(M(t),\lambda(t),g_i(t),\phi(t)...)}{dt}=0 \quad (51)$$

This scale invariance applies also to all order derivatives of V_{eff}^{RG} with respect to any of its parameters such as ϕ. Thus we also have the conditions:

$$\frac{d}{dt}\left(\frac{\partial V_{eff}^{RG}(M(t),\lambda(t),g_i(t),\phi(t)...)}{\partial\phi(t)}\right)=0 \quad (52)$$

and:

$$\frac{d}{dt}\left(\frac{\partial^2 V_{eff}^{RG}(M(t),\lambda(t),g_i(t),\phi(t)...)}{\partial^2\phi(t)}\right)=0 \quad (53)$$

The implication of these equations is that equations (24)-(26) from which we determine the state of occurrence of SSB and the resulting Higgs mass as well as signatures of REWSB (all arising from inherent dynamics of the system), have become independent of any one choice of renormalization scale t or M(t) at which we evaluate the system. In a way, V_{eff}^{RG} is now defined simultaneously over a whole range of the renormalization scale from $t=0$ to ∞, at any one point of which we can freely compute the dynamical quantities in equations (24) - (26) and determine at what points we have SSB and its corresponding mass spectra, unaffected by the value of the renormalization scale t at that point, except that the results obtained at any one t scale or point, differ from the results at another t scale or point by mere change or transformation of scale, but not intrinsic difference of dynamics of the system.

We note however that the above discussion regarding scale invariance of the RG improved effective potential holds strictly only where the potential

is not truncated as in equations (49) and (50). Where V_{eff}^{RG} is truncated and its arguments are evaluated with beta and gamma functions that are also computed only to a finite order (1-loop , 2-loop,... beta and gamma functions), equations (51)-(53) cease to hold exact. We correct for this by looking for a restricted stretch of the t scale, call it t^* with $t_1 \leq t^* \leq t_2$, where the truncated functions in equations (49) - (53) may still be considered reasonably flat or minimally dependent on t. We work with such flat regions for potentials (49)- (53), in place of the region $t = (0, \infty)$ of the exact scale invariant quantities. Now we analyze equations (49), (24)-(26).

Our first step is to compute the various running parameters of V_{eff}^{RG}, specified in equations (43) - (47). We illustrate our computational procedures by first considering the simpler case of 1-loop beta and gamma functions. Later we treat the case of 2-loop beta and gamma functions. To 1-loop beta and gamma functions [8], the running parameter equations to compute are:

$$g_1^2(t) = \frac{g_{01}^2}{1 - (41/48\pi^2)g_{01}^2 t} \tag{54}$$

$$g_2^2(t) = \frac{g_{02}^2}{1 + (19/48\pi^2)g_{02}^2 t} \tag{55}$$

$$g_3^2(t) = \frac{g_{03}^2}{1 + (7/8\pi^2)g_{03}^2 t} \tag{56}$$

with $g_{01} = 0.3407; g_{02} = 0.6585$ from equation (7) and $g_{03} = 1.23$.
Also we get values of $g_t(t), \lambda(t), \xi(t)$ by numerically integrating the following equations:

$$t = 16\pi^2 \int_{g_{t0}}^{g_t(t)} \frac{dg_t}{\frac{9}{2}g_t^3 - g_t[8g_3^2 + \frac{9}{4}g_2^2 + \frac{17}{12}g_1^2]} \tag{57}$$

$$t = 16\pi^2 \int_{\lambda_0}^{\lambda(t)} \frac{d\lambda(t)}{4\lambda^2 + B\lambda + C} \tag{58}$$

where $B = 12g_t^2 - 9g_2^2 - 3g_1^2$; and $C = -36g_t^4 + (9/4)g_1^4 + (9/2)g_2^2 g_1^2 + (27/4)g_2^4$. Here we use as boundary values, the pair of values $(\lambda_0 = 3.65464602; g_{t0} = 1.00605)$ from equation (34). Later we shall consider the other pair of values $(\lambda_0 = 0.002278; g_{t0} = 0.2513)$ of equation (33). Finally we have for the $\phi(t)$ and $\xi(t)$:

$$\phi(t) = \phi_0 \xi(t) = \phi_0 exp\left(-\frac{1}{16\pi^2}\int_0^t [3g_t^2 - \frac{9}{4}g_2^2 - \frac{3}{4}g_1^2]dt'\right) \tag{59}$$

with this integral separated into two parts for purposes of numerical computation :

$$\frac{1}{16\pi^2}\int_0^t [3g_t^2 - \frac{9}{4}g_2^2 - \frac{3}{4}g_1^2]dt' = \frac{1}{16\pi^2}\int_{g_{t0}}^{g_t(t)} [3g_t^2]dg_t(t') - \frac{1}{16\pi^2}\int_0^t [\frac{9}{4}g_2^2 + \frac{3}{4}g_1^2]dt' \tag{60}$$

We proceeded by assigning only positive values to scale t, and insisting in our numerical computations of equations (54) - (60) that we obtain only matching positive values of the coupling constants $g_1(t), g_2(t), g_3(t), g_t(t)$, and $\lambda(t)$. The results we obtained are shown in **figure 1**. The potential V_{eff}^{RG} equation (49) is next plotted against t, to search for a scale region t^* where V_{eff}^{RG} is reasonably flat, independent of t. From the plot shown in **fig. 2** we see that equation (49) is reasonably scale invariant in the region: $0 \leq t^* \leq 8$. This allows us to compute the quantities: $\partial V^{RG}/\partial\phi(t)$ and $\partial^2 V^{RG}/\partial^2\phi(t)$ at any point within this flat t^* region, and to run the quantities down to our reference scale $t = 0$. It is in this way that we obtain below, a Higgs (running) mass at the electroweak scale $t = 0$. The relevant quantities to compute and run in region t^8 are:

$$\frac{\partial V_{eff}^{RG}}{\partial\phi(t)} = 0 \tag{61}$$

implying a SSB condition any where in region t^* given by :

$$\lambda(t^*) + 4H(t^*)\left(log\frac{\phi^2(t^*)}{M^2(t^*)} - \frac{25}{6}\right) + 2H(t^*) = 0 \tag{62}$$

where :

$$H(t^*) = \left[\frac{12\lambda^2(t^*) - 3g_t^4(t^*)}{64\pi^2} + \frac{3(3g_2^4(t^*) + 2g_2^2(t^*)g_1^2(t^*) + g_1^4(t^*))}{1024\pi^2}\right] \tag{63}$$

Also :

$$\frac{\partial^2 V_{eff}^{RG}}{\partial^2\phi(t)} = m_h^2(t) \tag{64}$$

which combined with equation (62) gives within region t^*, a running Higgs mass of :

$$m_h^2(t^*) = 8\phi^2(t^*)H(t^*) \tag{65}$$

A plot of this $m_h^2(t^*)$ is shown in **figure 2** and yields a Higgs (running) mass value of $m_h = 245.6$ GeV at the electroweak scale t = $t^* = 0$. The corresponding physical Higgs mass differs from this by only a small vacuum polarization correction discussed by Casas et. al. [9,10] We will not go into

this.

Based on **figure 2**, we can interpret the region $t \geq 9.0$ not only as a region beyond which the 1-loop truncated RG improved effective potential is not reliable, but also as a cut off point Λ beyond which the Standard model EWSB theory is probably not valid. This will lead us to say that radiative electroweak symmetry breaking (REWSB) with RG improved effective potential (at 1-loop beta function) predicts a Higgs mass around 245.6 GeV, as well as a cut off energy scale $\Lambda \approx 8.0 \times 10^5$ GeV or less.

6 The Case $g_t > \lambda$ at electroweak scale

We examine next the features of REWSB in the case $g_t > \lambda$ at electroweak scale, presented by equation (33), in place of equation (34). We recall that equations (33) and (34) provided us a means to discriminate between two scenarios where at EWSB scale, the scalar field coupling λ is stronger (equation (34)) or weaker (equation (33)) than the top quark Yukawa coupling. Our calculations in sections 4 and 5, dealt with the case $\lambda_0 > g_{t0}$. Here we re-compute the same RG improved effective potential equation (49) under this alternative solution equation (33). Specifically we take as our new boundary values, the values given in equation (33): $\lambda_o = 0.002278$ and $g_{t0} = 0.25138$. We then re-compute our running parameters and the effective potential (49), together with the running Higgs mass. The results and features we find with equation (33) and the 1-loop beta and gamma function equations (43) - (47) are shown in **figure 3** . They lead us to a running Higgs mass of only 6.65GeV shown in **figure 4**. Since experiments already rule out such low mass Higgs boson, we can draw one conclusion that the REWSB model clearly selects only the solution (34): $\lambda_0 \gg g_{t0}$ at EWSB scale.

7 Case of 2-loop beta and gamma functions

Working now with only solution (34), we consider finally the case of 2-loop beta and gamma function RG improvement of the effective potential equation (49). According to Kastening [12],Bando et. al [13], one gets optimal improvement of a 1-loop effective potential if we evaluate it using 2-loop beta and gamma functions. We test this out by re-computing our REWSB

features and comparing with our 1-loop results of sections 4 and 5. Accordingly, we replace equations (54) to (60) by the following 2-loop beta function running parameters:

$$t = 16\pi^2 \int_{g_{01}}^{g_1(t)} \frac{dg_1(t)}{g_1^3\left[\frac{41}{6} + \frac{199}{18}g_1^2 + \frac{9}{2}g_2^2 + \frac{44}{3}g_3^2 - \frac{17}{6}g_t^2\right]} \tag{66}$$

$$t = 16\pi^2 \int_{g_{02}}^{g_2(t)} \frac{dg_2(t)}{g_2^3\left[\frac{-19}{6} + \frac{3}{2}g_1^2 + \frac{35}{6}g_2^2 + 12g_3^2 - \frac{3}{2}g_t^2\right]} \tag{67}$$

$$t = 16\pi^2 \int_{g_{03}}^{g_3(t)} \frac{dg_3(t)}{g_3^3\left[-7 + \frac{11}{6}g_1^2 + \frac{9}{2}g_2^2 - 26g_3^2 - 2g_t^2\right]} \tag{68}$$

with $g_{01} = 0.3407; g_{02} = 0.6585$ and $g_{03} = 1.23$ as before.
For 2-loop $g_t(t)$ and $\lambda(t)$,we compute positive values of the upper integration limits $g(t)$ and $\lambda(t)$ that match an assigned t value in the equations :

$$t = 16\pi^2 \int_{g_{t0}}^{g_t(t)} \frac{dg_t(t)}{-12g_t^5(t) + B_1 g_t^3(t) + C_1 g_t(t)} \tag{69}$$

and :

$$t = 16\pi^2 \int_{\lambda_0}^{\lambda(t)} \frac{d\lambda(t)}{-\frac{26}{3}\lambda^3(t) + B_2\lambda^2(t) + C_2\lambda(t) + D} \tag{70}$$

where :

$$\begin{aligned}
B_1 &= \frac{9}{2} + \frac{131}{16}g_1^2 + \frac{225}{16}g_2^2 + 36g_3^2 - 2\lambda \\
C_1 &= -8g_3^2 - \frac{9}{4}g_2^2 - \frac{17}{12}g_1^2 + \frac{1187}{216}g_1^4 - \frac{3}{4}g_2^2g_1^2 + \frac{19}{9}g_1^2g_3^2 - \frac{23}{4}g_2^4 + 9g_2^2g_3^2 - 108g_3^4 + \frac{1}{6}\lambda^2 \\
B_2 &= 4 - 24g_t^2 + 6(3g_2^2 + g_1^2) \\
C_2 &= 12g_t^2 - 9g_2^2 - 3g_1^2 - 3g_t^4 + 80g_3^2g_t^2 + \frac{45}{2}g_2^2g_t^2 + \frac{85}{6}g_1^2g_t^2 - \frac{73}{8}g_2^4 + \frac{39}{4}g_2^2g_1^2 + \frac{629}{24}g_1^4 \\
D &= -36g_t^4 + \frac{9}{4}g_1^4 + \frac{9}{2}g_2^2g_1^2 + \frac{27}{4}g_2^4 + 180g_t^6 - 192g_t^4g_3^2 - 16g_t^4g_1^2 - \frac{27}{2}g_t^2g_2^4 \\
&\quad + 63g_t^2g_2^2g_1^2 - \frac{57}{2}g_t^2g_1^4 + \frac{915}{8}g_2^6 - \frac{289}{8}g_2^4g_1^2 - \frac{559}{8}g_2^2g_1^4 - \frac{379}{8}g_1^6
\end{aligned} \tag{71}$$

The boundary values we use are from equation (34): $\lambda_0 = 3.65464602$ and $g_{t0} = 1.00605$. Also because of the greatly intertwined nature of the 2-loop β, γ functions and the running parameters, certain approximations had to be made in which quantities like B_1, B_2, C_1, C_2, D, in the above integrands, were treated as constants having values corresponding to a chosen t value,

or else to their known 1-loop values.

Finally for $\phi(t)$ and $\xi(t)$ we have the 2-loop gamma function equation:

$$\phi(t) = \phi_0 \xi(t) = \phi_0 exp\left(-\frac{1}{16\pi^2}\int_0^t [\gamma_1(t') + \gamma_2(t')]dt'\right) \tag{72}$$

where:

$$\begin{aligned}
\gamma_1(t) &= 3g_t^2(t) - \frac{9}{4}g_2^2(t) - \frac{3}{4}g_1^2(t) \\
\gamma_2(t) &= \frac{1}{6}\lambda^2 - \frac{27}{4}g_t^4 + 20g_3^2g_t^2 + \frac{45}{8}g_2^2g_t^2 + \frac{85}{24}g_1^2g_t^2 - \frac{271}{32}g_2^4 + \frac{9}{16}g_2^2g_1^2 + \frac{431}{96}g_1^4
\end{aligned} \tag{73}$$

The results of computing these 2-loop running parameters, and plugging into equations (49), (24) - (26), are shown in **figures 5 and 6.** Some individual running parameters appear greatly modified at the 2-loop level. This is particularly so for $\lambda(t)$ and $g_2(t)$ seen from figures 1 and 6. Correspondingly, the 2-loop RG improved effective potential does not exhibit much of a flat t^* region seen in figure 6 compared to 1-loop figure 2. The value of running Higgs mass at EWSB scale :$t = 0$ predicted in both cases is however about the same : $m_h = 245.6$ GeV.

8 Relating our results to other calculations

We can compare these features of our RG improved REWSB with features found in conventional electroweak symmetry breaking calculations. We already showed in section 3 that CEWSB (at tree level), does not predict any explicit value of the Higgs mass m_h nor the scalar coupling constant λ. But the conventional electroweak symmetry breaking potential (with $\mu^2 \neq 0$) can also have higher order potential terms added to it as in equation (16), and treated to a RG group improvement as for our REWSB model considered in sections 5 and 6. This has been done by a number of authors [7-17], particularly Ford et. al. [8] and Casas et. al. [9,10]. We can look at these RG improved CEWSB results and compare them to our REWSB results to see any particular signature features. These authors [8-10] worked with 1-loop effective potential of the form shown in equations (27) and (50) to which non-zero scalar field mass term $\mu^2 \neq 0$ is added from equation (1). This RG improved CEWSB equation (50) is then analyzed by the usual equations (24) - (26), combined with the additional requirement of vacuum

stability or $\lambda \geq 0$. Casas et. al [9,10] obtained a Higgs mass estimate of $m_h > 128 \pm 33$GeV, to be compared with our explicit REWSB result of running Higgs mass $m_h = 245.6$ GeV. Admittedly, many of these CEWSB RG improved effective potential analysis, were done at a time the top quark mass was still considered unknown free parameter, in contrast to our treatment. Ford et. al. [8] for example stated their result in terms of the top quark mass : $m_h \geq 1.95 m_t - 189$GeV. Overall, there appears a need to re-analyze the RG improved CEWSB effective potential case for better comparison with REWSB, and to ascertain the role the scalar field mass parameter $\mu \neq 0$ actually plays.

Another comparison we can make is with the recent work of Elias et. al.[2-6] who analyzed the same radiative electroweak symmetry breaking (REWSB), and raised the same issue of the possible experimentally accessible signature differences of REWSB and CEWSB. They worked not with the standard Coleman-Weinberg Feynman loop calculated effective potential equations (15), (23), (27), (49), (50), but took advantage of the fact that the loop calculated effective potentials invariably involved leading logarithms as in equation (20), multiplied by a factor C that involves products of EW coupling constants and the scalar field ϕ. Elias et. al. showed that this usual Coleman-Weinberg RG improved effective potential in the particular case of REWSB can be realized as a direct summation to infinity of leading logarithm terms. Putting such leading logarithm parameterized effective potential through the usual equations (24) - (26), Elias et. al. obtained a REWSB Higgs mass ranging in value from $m_h = 216 - 231$ GeV. They obtained ssociated scalar field coupling $\lambda = 2.15$. These results are comparable to our values $m_h = 245.6$ GeV, and $\lambda = 3.65$. Their values for other EW coupling constants are also very comparable, Thus while for the top quark, Elias et. al. obtained the value $g_{t0} = 1.00$ at EWSB scale, we obtained in equation (34) the value $g_{t0} = 1.00605$.

9 Summary and Conclusions

. We find close agreement between our results based on the standard Coleman-Weinberg loop calculated, and renormalization group improved, effective potential, and the Elias et. al. results based on direct summation of leading logarithm terms. Basing on both calculations of the same radiative electroweak symmetry breaking (REWSB), we can re-affirm that REWSB model

not only remains a viable mechanism of electroweak symmetry breaking, but is able to give an explicit value of the (running) Higgs mass. The (running) Higgs mass predicted by the REWSB mechanism, lies in the range 215 - 250 GeV, at electroweak scale. In contrast the CEWSB models of Ford et. al [8], Casas et al. [9.10] and others [7,14-16], are only able to put a lower bound typically $m_h \geq 1.95 m_t - 189\text{GeV}$ on the Higgs mass. Because of this limited information from CEWSB, we cannot use the Higgs mass value as a conclusive signature to distinguish between REWSB from CEWSB.

We are left to consider the coupling constants λ and g_t of the system. Our calculations established two points regarding λ and g_t. We found that of the two possibilities : $\lambda > g_t$ or $g_t > \lambda$ at EWSB scale, the $\lambda \gg g_t$ is the correct one, while the case $g_t > \lambda$ that implies a Higgs mass $m_h \approx 6.65 GeV$ is already ruled out by experiment. Explicitly, we obtained in our equation (34) that the ratio $\lambda/g_t = 3.63$. Elias et. al. found a lower ratio of 2.15. The two results are however consistent to the extent $\lambda \gg g_t$.

If we accept the REWSB value of Higgs mass of 215 - 250 GeV as physical Higgs mass holding whether the mechanism of EWSB is by REWSB or by CEWSB, we can deduce the corresponding λ_{CEWSB} value from equations (13) and (14). We find $\lambda_{CEWSB} = 0.997$ to be compared with $\lambda_{REWSB} = 3.65$ at the same Higgs mass of 245.6 GeV. We conclude as did Elias et. al. [2,3], that the REWSB mechanism is associated with a greatly enhanced scalar field coupling $\lambda_{REWSB} \gg \lambda_{CEWSB}$.

This can become an important signature difference between REWSB and CEWSB that can be verified experimentally. The fact is that based on equations (1) and (2), the individual scalar field components $\phi_1^+, \phi_2^+, \phi_4^o, \phi_3^o$ all couple with the same strength, λ_{CEWSB} or λ_{REWSB} depending on the model. When this fact is combined with the equivalence theorem [18] between EWSB Nambu-Goldstone bosons and linearly polarized gauge bosons, one comes to the conclusion that interactions of W_L^+, W_L^-, Z_L^o can provide experimentally observable coupling constant based signature differentiation between REWSB and CEWSB, a fact pointed out by Elias et. al. [2,3], but needing further study.

The observed enhanced coupling $\lambda_{REWSB} \gg \lambda_{CEWSB}$ by itself calls for explanation. It suggests as part of our main finding that the scalar field couples less strongly to achieve the same end result of EWSB in a quantum system that has a pre-set mass scale $\mu^2 \neq 0$, compared to the same quantum

system with no pre-set scale $\mu^2 = 0$. The same scalar field couples more strongly in the latter case. Whether this is a general principle of quantum dynamics is something for further study.

References :

1. S. Coleman and E. Weinberg, Phys. Rev. D7 (1973) 1888 .

2. V. Elias, R.B. Mann, D.G.C.McKeon, and T.G. Steele, Phys. Rev. Lett. 91, 251601.

3. F. A. Chishtie, V. Elias, and T. G. Steele, Intern. Journ. Mod. Phys. A20 (2005) 6241.

4. V. Elias, R.B. Mann, D.G.C. Mckeon and T.G. Steele, Nucl. Phys. B678 (2004) 147.

5. V. Elias, R. B. Mann, D.G.C. McKeon and T.G. Steele, arXiv.hep-ph/0508107 (2005).

6. F. A. Chistie, V. Elias, R.B. Mann, D.G.C.McKeon, and T.G. Steele, Nucl. Phys. B 743 (2006) 1034.

7. M. Sher, Phy. Report 179 (1989) 273.

8. C.Ford, D.R.T.Jones, P.W Stephenson and M B Einhorn, Nucl. Phys.B395 (1993) 17.

9. J.A. Casas, J.R. Espinosa, M. Quiros and A. Riotto, Nucl. Phys. B436 (1995) 3; (E) B439 (1995) 466.

10. J.A. Casas, J.R. Espinosa, M. Quiros, Phys. Lett. B342 (1995) 171.

11. T. P. Cheng and L. F. Li , Gauge theory of elementary particle physics, Oxford University Press (1984).

12. B. Kastening : Phys. Lett. B283 (1992) 287.

13. M. Bando, T. Kugo, M. Maekawa and H. Nakano, Phys. Lett. B301 (1993) 83 ; Prog. Theor. Phys. 90 (1993) 405.

14. G. Altarelli and G. Isidori Phys. Lett. B 337 (1994) 141

15.M. Lindner, M. Sher and H.W. Zaglauer, Phys. Lett. B228 (1989) 139.

16. Vincenzo Branchina and Hugo Faivre, Phys. Rev. D72 (2005) 065017.

17. P. Kielanowski, S.R. Juarez W, and H.G. Solis-Rodriguez, Phys. Rev. D72 (2005) 096003).

18. P. N. Maher, L. Durand and K. Riesseimann, Phys. Rev. D 48 (1993) 1061.

Figure Captions:

Figure 1 : Running parameters of RG improved effective potential at 1-loop β and γ functions and for equation (34), $\lambda_o > g_{t0}$.

Figure 2 : Flatness t^* test and running Higgs mass plot yielding a running Higgs mass intercept of $m_h = 245.6$ GeV at EW scale t = 0.

Figure 3 : Running parameters of RG improved effective potential at 1-loop β and γ functions, with $g_{t0} > \lambda_o$, equation (33) case.

Figure 4 : Flatness t^* and running Higgs mass plots at 1-loop β and γ functions, and for $g_{t0} > \lambda_o$ equation (33) case.

Figure 5 : Running parameters of RG improved effective potential at 2-loop β and γ functions and for equation (34), $\lambda_o > g_{t0}$.

Figure 6 :2-loop β and γ functions flatness t^* and running Higgs mass plots, yielding a running Higgs mass intercept of $m_h = 245.6$ GeV at EW scale t = 0.

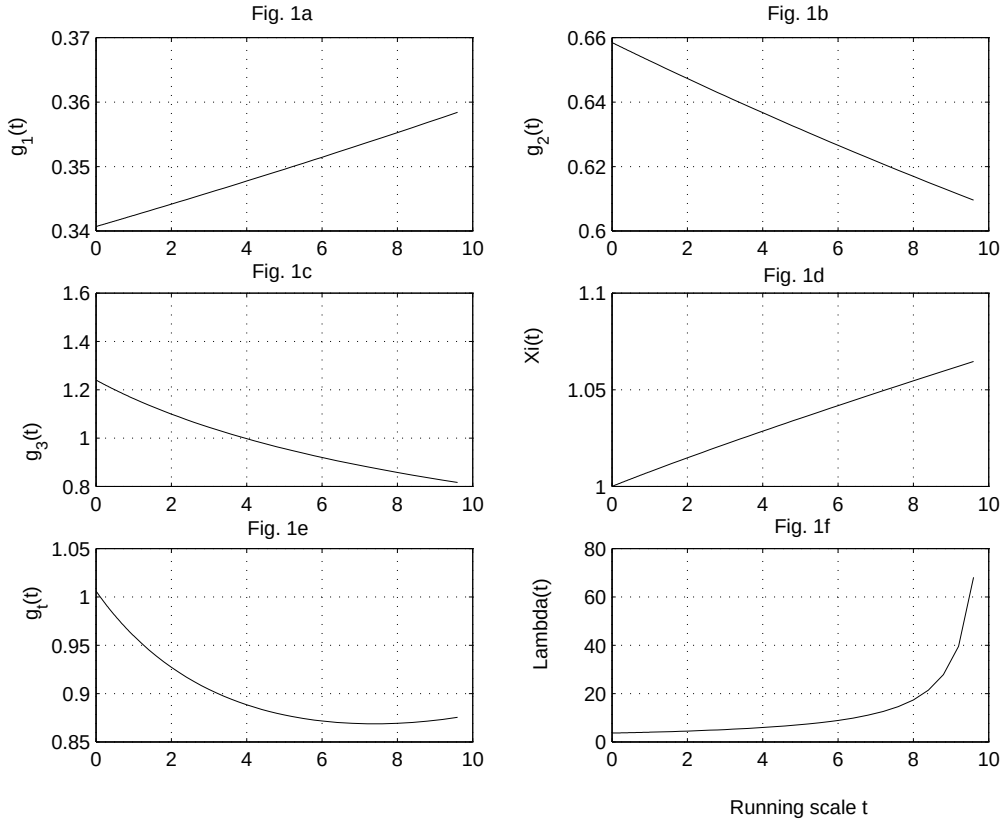

Figure 1: Running parameters of RG improved effective potential at 1-loop β and γ functions and for equation (34), $\lambda_o > g_{t0}$.

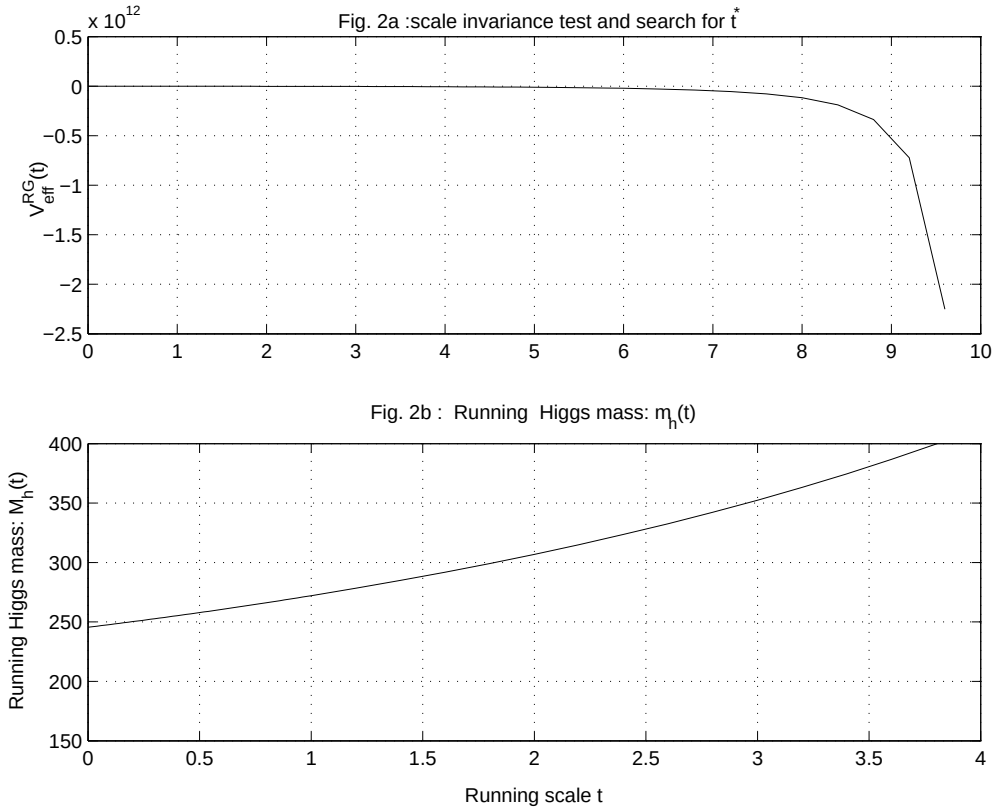

Figure 2: Flatness t^* test and running Higgs mass plot yielding a running Higgs mass intercept of $m_h = 245.6$ GeV at EW scale t = 0.

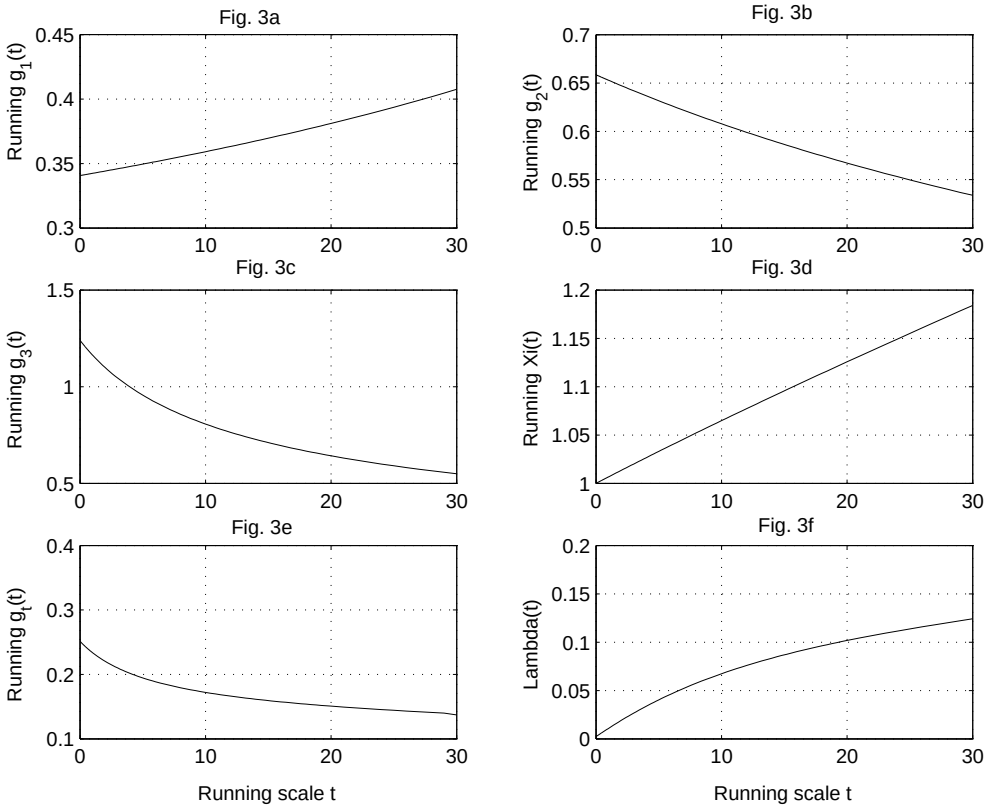

Figure 3: Running parameters of RG improved effective potential at 1-loop β and γ functions, with $g_{t0} > \lambda_o$, equation (33) case.

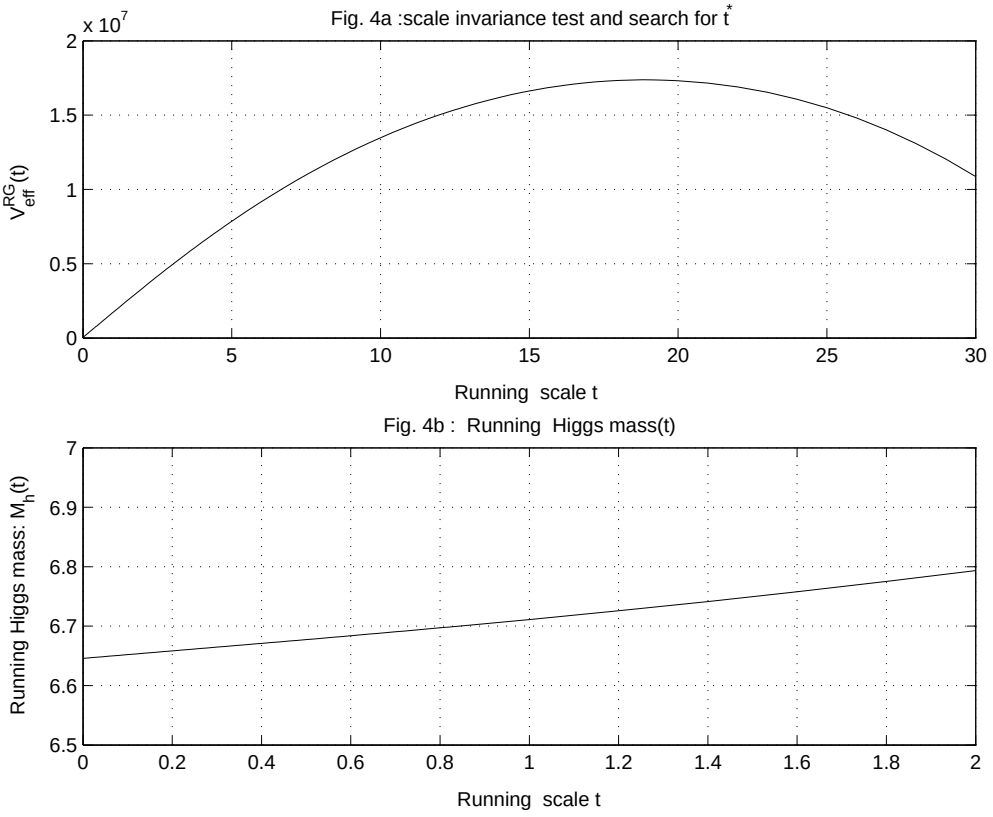

Figure 4: Flatness t^* and running Higgs mass plots at 1-loop β and γ functions, and for $g_{t0} > \lambda_o$ equation (33) case.

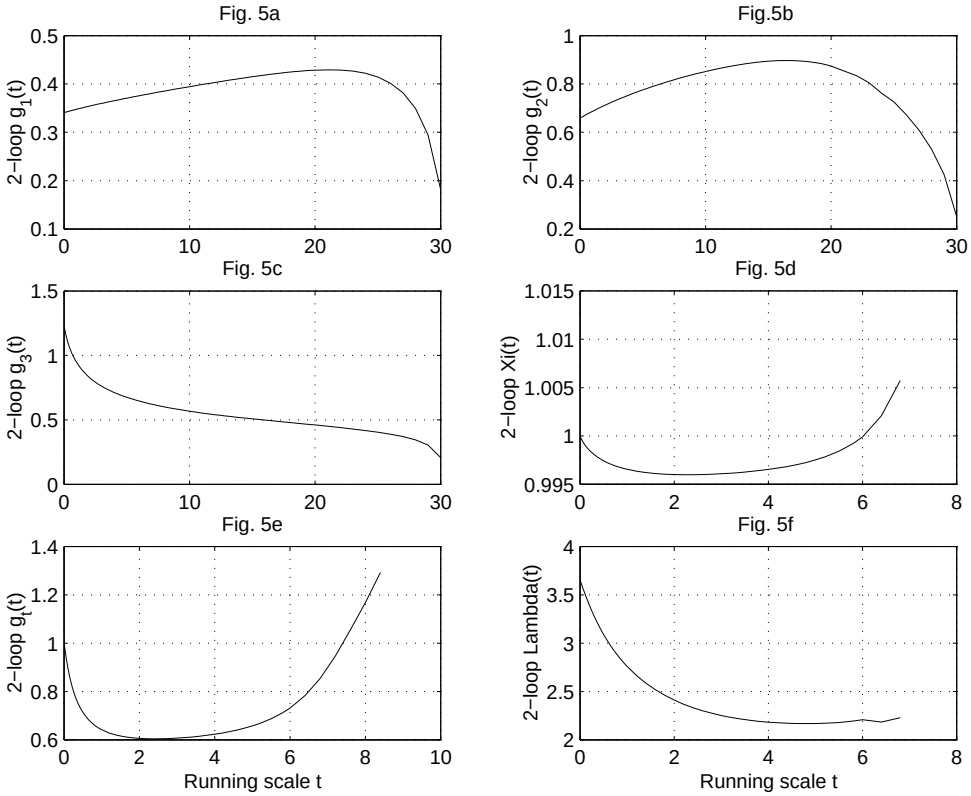

Figure 5: Running parameters of RG improved effective potential at 2-loop β and γ functions and for equation (34), $\lambda_o > g_{t0}$.

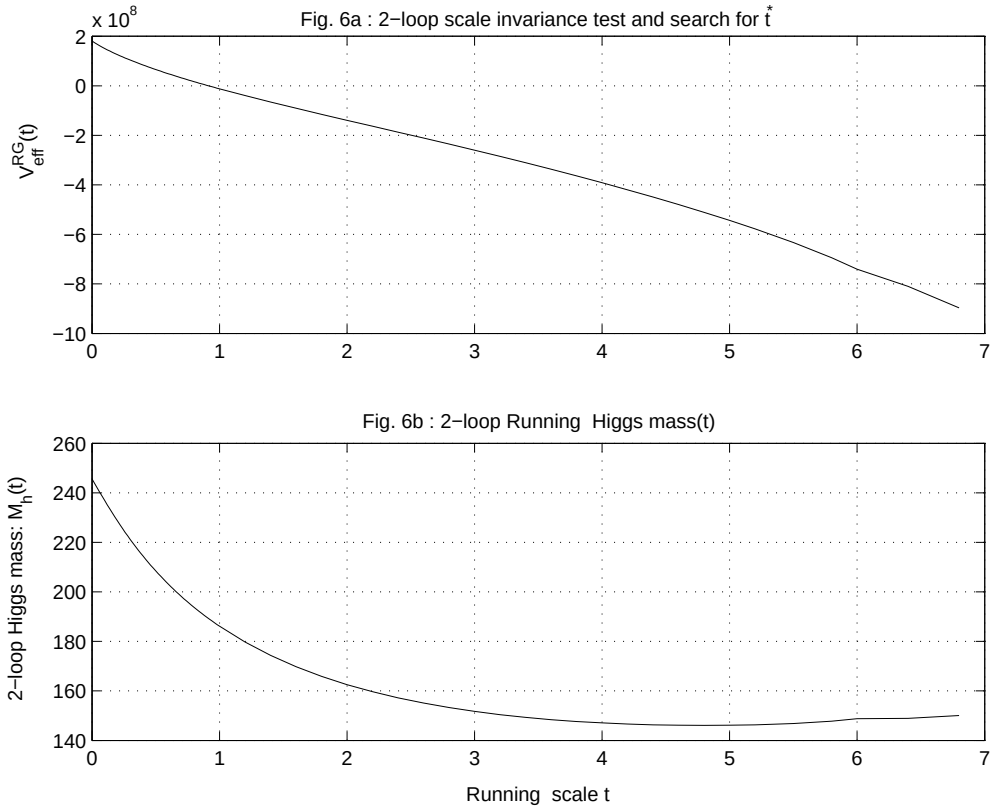

Figure 6: 2-loop β and γ functions flatness t^* and running Higgs mass plots, yielding a running Higgs mass intercept of $m_h = 245.6$ GeV at EW scale t $= 0$.